A Journal of the Gesellschaft Deutscher Chemiker

Angewandte International Edition Chemie

GDCh

www.angewandte.org

Accepted Article

Title: Organic Nanocrystals with Bright Red Persistent Room-Temperature Phosphorescence for Biological Applications

Authors: Seyed Mohammad Ali Fateminia, Zhu Mao, Zhiyong Yang, Shidang Xu, Zhenguo Chi, and Bin Liu

To be cited as: *Angew. Chem. Int. Ed.* 10.1002/anie.201705945
Angew. Chem. 10.1002/ange.201705945

Link to VoR: http://dx.doi.org/10.1002/anie.201705945
http://dx.doi.org/10.1002/ange.201705945

WILEY-VCH

10.1002/anie.201705945

WILEY-VCH

Organic Nanocrystals with Bright Red Persistent Room-Temperature Phosphorescence for Biological Applications

S. M. Ali Fateminia[†] [a], Zhu Mao[†] [b], Shidang Xu [a], Zhiyong Yang* [b], Zhenguo Chi* [b], Bin Liu* [a]

Abstract: Persistent room-temperature phosphorescence (RTP) in pure organic materials has attracted great attention due to their unique optical properties. The design of organic materials with bright and red persistent RTP remains challenging. Herein, we report a new design strategy for realizing high brightness and long lifetime of red-emissive RTP molecules, which is based on introducing an alkoxy spacer between the hybrid units in the molecule. The spacer offers easy Br-H bond formation during crystallization, which also facilitates intermolecular electron coupling to favor persistent RTP. As majority of the RTP compounds have to be confined in a rigid environment in order to quench non-radiative relaxation pathways for bright phosphorescence emission, nanocrystallization is used to not only rigidify the molecules, but also offer the desirable size and water-dispersity for biomedical applications.

Pure organic materials with persistent room-temperature phosphorescence (RTP) are an advantageous alternative to their organometallic counterparts. This is mainly because they are considerably cheaper, environmentally safer and biologically more compatible, allowing a wide range of optical, electronic and biological applications, such as electroluminescence, data storage, molecular sensing and time-resolved bioimaging.[1-3] As opposed to loosely-bonded electrons in organometallic materials, the highly bonded nature of electrons in pure organic materials restricts their ability to decay through radiative relaxation pathways from triplet states. Therefore, triplet states in organic materials are prone to non-radiative relaxations through thermal and collisional processes.[4] In addition, the triplet states are easily quenched by atmospheric oxygen molecules via triplet-triplet energy transfer. As such, intense phosphorescent materials are largely known to exist in inert gas and at very low temperatures, which in turn limits their practical applications.[5] Recently, researchers discovered several examples of pure organic materials that exhibited persistent phosphorescence in air and at room temperature.[6-13] These discoveries sparked several attempts to find a general strategy to design more of such materials for various applications. It was found that, to yield efficient RTP, several key factors have to be considered. The first is to promote intersystem crossing (ISC), and the second is to suppress the non-radiative relaxation pathways such as intermolecular motions.[14, 15] To promote ISC and to favor pure organic RTP, heavy halogen atoms, as well as organic groups with lone electron pairs, such as aromatic carbonyls, have been successfully introduced to organic compounds.[16-19] However, our ability to quench the non-radiative processes of organic compounds remains limited.[20] So far, several strategies have been applied to minimize the intermolecular and intramolecular motions to activate the phosphorescence emission, which include host–guest doping systems with supra-molecular gel entrapping,[21] metal-organic framework coordination[22] and rigid solid protection,[4] polymer assistance,[23, 24] and crystal formation.[16] Except for the crystallization approach, additional molecules or matrices are always involved in the rigidification methods, which add complexity to their applications with compromised performance due to the diluted RTP molecule concentration. This is particularly a concern in biological applications as the biocompatibility and negligible interference between the matrix and the biosystem must be ensured which adds further limitations to the design. Therefore, crystal formation is a rather ideal strategy to bring RTP materials into biological applications. Since the first report on crystallization induced phosphorescence emission from pure organic compounds (*i.e.* benzophenone and its derivatives) at room temperature,[16] the number of organic compounds showing CIP (crystallization-induced phosphorescence) has gradually expanded in the past few years.[4] However, all these crystals are too large in size for biological applications, and the majority of the RTP compounds with high brightness are more or less limited to short wavelength emissions, which hampers their bioimaging applications.[25-27]

It is well-known that long-lasting luminescence and good biocompatibility are highly desirable for *in-vitro* and *in-vivo* imaging without the interference of autofluorescence. Despite the fact that RTP materials have proven to have such qualities, there are very few successful attempts to bring them into biological systems.[28] This is because compounds with long-wavelength emission are generally needed to overcome the bio-substrate auto-fluorescence. In addition, a strategy should be available to control the crystal size to nanometer range so that they become compatible with biological systems. Moreover, the obtained nanocrystals should remain emissive as the oxygen molecules dissolved in the aqueous media can effectively quench their phosphorescence. This further requires the quantum yield of the RTP molecules to be high enough so that they can remain emissive when they are well-dispersed in aqueous media.[29]

One of the first attempts to produce red-emissive RTP materials was done by Bolton *et al*, based on planar naphthalene derivatives. To promote ISC, aromatic carbonyl and heavy halogen atoms were incorporated in the structure. The lifetime and efficiency of the red-emissive crystals are 0.6 ms and 1%, respectively. Due to self-quenching of the molecule, crystallization has to be done in a host-guest system, reducing the quantity of the molecule in crystals to be only 1%.[4] To address the limitations of self-quenching and the need of using a host-guest system, An *et al* designed a non-planar structure comprised of a phenylphosphine and two carbazolyl groups. Two factors were considered in their design in order to yield higher brightness and longer lifetime. Firstly, O, N and P atoms were used to favor ISC transition, thanks to the lone-pair electrons. Moreover, substituents were included in the chemical structure to enhance the formation of *H*-aggregates, which stabilized the triplet excited state, and therefore increased the lifetime. The resulting pure phosphorescent crystals showed red emission with a long lifetime of more than 1 s. However, the quantum yield of the crystals was only around 2%.[6] Later, Yang *et al* further increased the quantum yield of red organic RTP compounds to 5% by combining the heavy halogen atom effect

[a] S. M. A. Fateminia, S. Xu, Dr. B. Liu
Department of Chemical and Biomolecular Engineering
National University of Singapore
4 Engineering Drive 4, Singapore, 117585 (Singapore)
E-mail: cheliub@nus.edu.sg
[b] Z. Mao, Dr. Z. Yang, Dr. Z. Chi
PCFM Lab, GDHPPC Lab, Guangdong Engineering Technology Research Center for High-performance Organic and Polymer Photoelectric, Functional Films, State Key Laboratory of OEMT
School of Chemistry
Sun Yat-sen University, Guangzhou 510275 (China)
E-mail: yangzhy29@mail.sysu.edu.cn; chizhg@mail.sysu.edu.cn
[†] S. M. A. Fateminia and Z. Mao contributed equally to this work.

Supporting information for this article is given via a link at the end of the document.

and intermolecular electronic coupling (IEC). They showed that it was possible to combine the advantages of n and π units through electronic coupling of two adjacent molecules, which in turn produced hybrid ISC transitions and resulted in bright long-lived RTP.[11]

In this contribution, we report a new design strategy to modulate the IEC and the heavy atom effects independently by simply introducing a soft proper alkoxy spacer group between the hybrid units for long-lived and highly emissive red RTP. The nanocrystals of the compound were further produced to demonstrate their potentials in biological applications. The molecular design starts from a reported persistent RTP molecule, C-Br, which is one of the brightest red phosphorescent compounds reported so far.[11] C-Br has a persistent phosphorescence emission at 549 nm with a lifetime of 280 ms, benefiting from the strong IEC effect. [10, 11] To further improve the brightness of red RTP, a stronger heavy halogen atom effect is desired, which can be achieved through the formation of a stronger bond between the bromine atom of one molecule and the carbazolyl plane of the neighboring molecule in the crystalline form. A soft butoxy spacer is thus introduced into C-Br thereby spatially separating the carbazole and the 4-bromobenzophenone groups to offer the new molecule (C-C4-Br) with a higher level of conformational flexibility (Scheme 1). Such a change is expected to facilitate the bond formation between the head of one molecule and the tail of the other in the crystalline form, leading to a more efficient IEC [11] and intermolecular heavy halogen effect.[30]

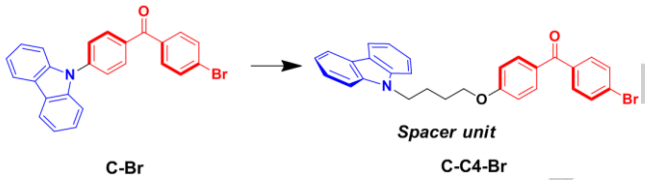

Scheme 1. The molecular design strategy for a red RTP compound with high efficiency and long lifetime.

The synthetic route to C-C4-Br is shown in Figure S1. C-C4-Br was obtained in 90% yield after four steps of reactions from 4-bromo-4'-hydroxybenzophenone and 9-(4-bromobutyl)-9H-carbazole. ^{1}H, ^{13}C NMR and high resolution mass (HRMS) characterization reveal that the final product and the intermediates are of right structures with high purity (Figures S2-S4). The absorption and photoluminescence (PL) spectra of C-C4-Br in tetrahydrofuran (THF) solution are shown in Figure S5. It has an absorption maximum at 350 nm; however, no detectable emission is observed due to the dominance of non-radiative relaxation pathways of C-C4-Br in solution. On the other hand, the PL spectrum of C-C4-Br in crystalline powders has two clear peaks at 570 and 620 nm. The position of emission peaks is similar to C-Br; however, C-C4-Br crystals are clearly brighter. To further explore the effect of crystallization on molecular configuration, single crystal structure analysis is performed. The results of crystal structure analysis in Figures 1a and S6 reveal that both crystals of C-Br and C-C4-Br exhibit strong IEC effect represented by the dashed green lines. In C-Br, this effect exists between the carbonyl group of one molecule and the carbazolyl group of the adjacent molecule; while in C-C4-Br, it happens between the two different carbazolyl groups of two neighboring molecules. The similar packing is also found in carbazole crystals with a distance of 3.716 Å between molecules (Figure S6a). The shorter distances between the carbazole rings for the coupled C-C4-Br molecules (3.421 and 3.538 Å, green dashed lines in Figure 1a) indicate stronger intermolecular interactions in C-C4-Br crystals. Despite the similarity in the IEC effect, the heavy halogen atom effect is different in the two crystals. The CBr bond in the C-Br crystal is far from the adjacent carbazolyl plane and points nearly parallel to it (dashed purple line, Figure S6), which in turn weakens the effect of heavy halogen atom on carbazolyl unit. In contrast, the CBr bond in C-C4-Br crystal directs almost vertically to the adjacent carbazolyl plane (dashed purple line, Figure 1a). Moreover, the bromine atom is located in close proximity of the C=C bond in the carbazolyl group (dashed orange line with the length of 3.429 Å, Figure 1a). To explore the effect of such stronger bond formation on the emission properties of C-C4-Br, the luminescence spectra of the crystals were measured under steady-state and delayed mode (30 ms delay) (Figure 1b). The results reveal that at room temperature, the only emissive pathway in C-C4-Br crystals is phosphorescence. The new design results in more than 200% enhancement in the phosphorescence quantum efficiency of C-C4-Br (11%) as compared to C-Br (5%). Considering the long phosphorescent lifetime of 0.14 s is observed for C-C4-Br, it represents one of the most efficient red-emissive persistent RTP materials reported so far.

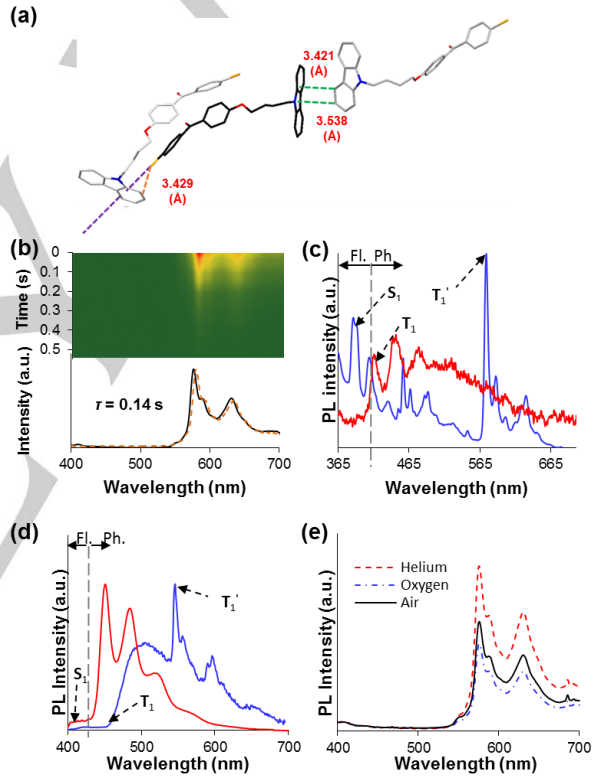

Figure 1. (a) Positioning of C-C4-Br molecules in the single crystal structure (b) The steady state and persistent (delay 30 ms) luminescence spectra of C-C4-Br crystal at room temperature; The PL spectra of (c) C-C4-Br and (d) C-Br in different states at 77K: diluted solution in 2-methyl-tetrahydrofuran (red curve) and crystal powder (blue curve). Fl. = fluorescence, Ph. = phosphorescence, S_1 = the lowest singlet excited state, T_1 = the lowest triplet excited state of mono-molecule in crystal powder. T'_1 = the lowest triplet excited state of the IEC hybrid units for the persistent RTP in crystal; (e) the PL spectra of C-C4-Br large crystals in different environments.

As shown in Figures 1c and 1d, despite enhancement of the long-lived phosphorescent peaks, new phosphorescent peaks are presented in their PL spectra of both crystal samples of C-Br and C-C4-Br at low temperature (77K), due to the suppression of competitive non-radiative thermal decay process. To understand the origin of phosphorescence emissions from C-C4-Br crystals at 77 K, the RTP photos and the phosphorescence (delay) spectra of carbazole, 4-bromo-4'-methoxyl-benzophone (BMB) and C-C4-Br samples are shown

in Figures S8 and S9, respectively. It was found that carbazole, BMB and C-C4-Br exhibit RTP only in crystals, and no RTP is observed in either solution state or when the molecules are doped in Zeonex films, revealing that the intramolecular interaction itself does not lead to RTP. Detailed analysis also reveals that the RTP in C-C4-Br crystals is dominated by the carbazole emission at room temperature, as they share the similar emission spectra while the characteristic peak at 510 nm for BMB crystals is not visible in the RTP spectrum of C-C4-Br. When the C-C4-Br crystals are cooled to 77 K, the phosphorescent emission is still dominated by the carbazole molecules, but the emission peaks from 420-500 nm seem to resemble that of molecular emission (particularly BMB emission as carbazole does not give noticeable phosphorescence as molecular species).

Figures S10 and S11 are frontier orbitals associated with ISC. Different from the isolated C-C4-Br molecules, where the HOMO and LUMO are clearly localized on the carbazole and BMB, respectively, the HOMO and HOMO-2 orbitals are dispersed on both carbazole groups of the two coupled C-C4-Br molecules in crystals, which indicate intermolecular components in the relative intersystem crossing channels. Furthermore, the most major possible ISC channel for coupled C-C4-Br molecules (Figure S12, from HOMO to LUMO) is an intermolecular process, which transfers from carbazole of one C-C4-Br to BMB of an adjacent molecule. These results reveal that IEC effect plays an important role in yielding high RTP in C-C4-Br crystals.

For biological applications, the exposure of RTP materials to O_2 is inevitable. As O_2 is a strong quencher of the excited triplet state, the compound needs to be bright enough to remain emissive even after being partly quenched by O_2 present in the aqueous medium. Therefore, the influence of oxygen on the persistent RTP of the C-C4-Br crystals was further explored. As shown in Figure 1e, the bulk crystal powders show some sensitivity to oxygen. Both the emission intensity and lifetime reduce slightly after the environment is changed from helium to air (Figures 1e and S13a). The decrease is even more obvious when the crystals were exposed to oxygen. This is a clear indication that the O_2 molecules can quench the triplet excitons.

To make the crystals suitable for biological applications, their sizes have to be adjusted to sub-micro range. In this case, a nanocrystallization strategy is applied to obtain very small size crystals.[29] The nanocrystallization method is based on ultrasonication of the amorphous nanoaggregates of the compound in a solvent/anti-solvent medium (*e.g.* THF/water) in which crystallization can happen. As higher fraction of the antisolvent can be effective in decreasing the crystal size, a morphological study in mixtures of different THF/water ratios was conducted first in order to obtain the proper volume fraction of water (f_w) for nanocrystallization. Starting with f_w = 80%, the initially formed particles are amorphous nanoaggregates (Figure S10b). After storage for a day, micrometer-long ribbon-like C-C4-Br crystals emerge (Figure S10d). A higher f_w of 85% still results in the formation of ribbon-like crystals after 3 days storage (Figure S10c), which appear to be smaller than those formed at f_w = 80%. This is due to the decreased crystal growth rate resulted from the higher antisolvent fraction. However, raising f_w to 90% does not cause any further size reduction, but rather amorphous nanoaggregates remain intact (**Figure 2a**) due to domination of anti-solvent to solvent properties.[29] Therefore, f_w = 85% is chosen as the medium in nanocrystallization with the assistance of ultrasound waves. Starting from the amorphous nanoaggregates in the medium, the PL spectrum of the suspension is recorded regularly to monitor the crystallization process (Figure 2b). It is found that the two phosphorescence peaks appear after 30 s of ultrasonication. The PL intensity grows by time, showing that more amorphous particles are converted to nanocrystals; however, it does not change significantly after 120 s, indicating that all the amorphous nanoparticles are converted to nanocrystals. Therefore, 120 s is taken as the optimum treatment time for nanocrystallization. The peaks in the PL spectrum of nanocrystals in suspension are almost the same as solid powder of bulk crystals (Figure 2d), showing that neither nanocrystallization nor dispersion in aqueous medium could completely quench the phosphorescence emission of C-C4-Br. Morphology studies reveal that the nanoaggregates before treatment have the same shape and diffraction pattern as amorphous nanoaggregates formed at f_w = 90% with an average size of 80 nm (Figure S14). However, after 120 s treatment, the particles form rod-like structures with a slight increase in size to 180 nm (Figure 2c). The crystallinity of single nanocrystal is confirmed by (SAED) pattern (inset of Figure 2b). The formation of nanocrystals in solid state is further evidenced with their XRD spectrum after treatment (Figure 2e). A similar trend is also observed in C-Br nanocrystallization process (Figure S15), however, the C-Br nanocrystals are only emissive in solid state, and no emission is detected in aqueous medium. The difference between C-C4-Br and C-Br as nanocrystals is due to the higher quantum yield of C-C4-Br, which makes it glow even after being partially quenched by water and oxygen molecules. Quantitative measurements performed on nanocrystals of C-C4-Br reveal a larger degree of phosphorescence quenching in the presence of O_2 as compared to bulk crystals. This can be attributed to the higher surface to volume ratio in nanocrystals, and therefore a larger fraction of atoms are available to be exposed directly to the environment to partially quench the luminescence (Figures S13b and 13c), yet the C-C4-Br nanocrystals remain quite emissive. As emission in aqueous media is crucial for bringing the phosphorescence properties into biological applications; the rest of the study is mainly focused on C-C4-Br.

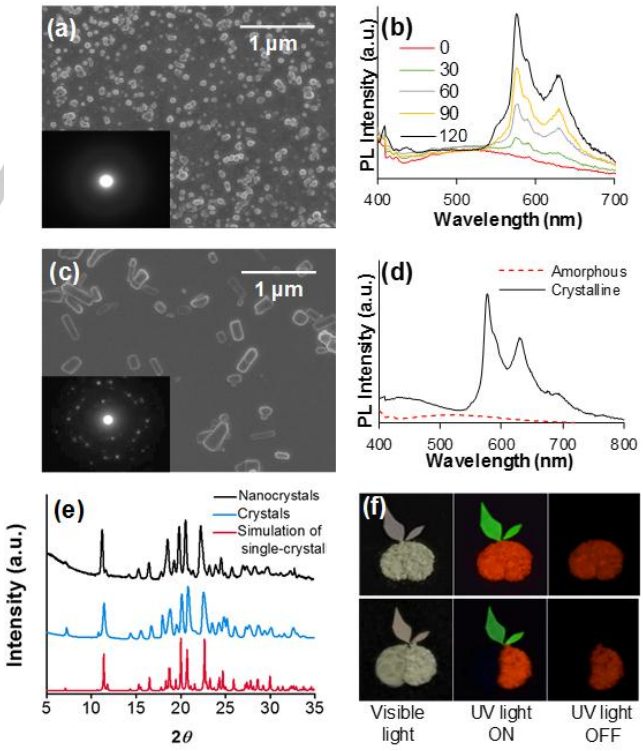

Figure 2. SEM images of (a) amorphous nanoaggregates formed in f_w = 90% and (b) at different treatment time in suspension (c) nanocrystals with their respective SAED pattern as inset; PL spectra of C-C4-Br nanoparticles (d) in solid-state; (e) XRD spectrum of C-C4-Br nanocrystals, crystal powders and

simulation form the single crystal data; (f) the luminescence of nanocrystals and amorphous nanoaggregates of C-C4-Br (the orange body) and fluorescein (the leaves) under different illumination conditions.

Figure 2f demonstrates the persistent phosphorescence emission of the C-C4-Br at room temperature. In the first row, one starts with an orange fruit made of C-C4-Br nanocrystals and leaves made of fluorescein. In the second row, half of the orange on the left is substituted with amorphous nanoaggregates of C-C4-Br. There is not any obvious difference between the two orange fruits under visible light, however, under 365 nm UV irradiation, the difference becomes evident. Nanocrystalline parts of the orange as well as the fluorescein leaves are emissive while the amorphous part of the fruit does not show any emission, which is in accordance with PL measurements described earlier. After turning the UV light off, the fluorescent leaves turn off immediately, leaving the phosphorescence emission from the orange fruit to emit which is clearly visible by naked-eye.

The C-C4-Br nanocrystals and amorphous nanoaggregates were applied for bioimaging of 231 breast cancer cells to demonstrate their potential biological applications. Although time-gated microscopy is the best option to differentiate auto-fluorescence from the phosphorescence emission, the lifetime of C-C4-Br is several orders of magnitude longer than the detection limit of time-gated microscopes. Therefore, we collected the cells labelled with C-C4-Br nanocrystals and show that the RTP can be effectively used to differentiate the cells from the fluorescein fluorescence interference (Figure 3). In addition, a confocal laser scanning microscopy (CLSM) was used to perform the imaging process. Figures 3a-3d show images of cells incubated with both amorphous nanoaggregates and nanocrystals. No emission signal is observed from cells incubated with amorphous nanoaggregates; however, a bright phosphorescence emission in the red channel is collected for the well-internalized nanocrystals. Moreover, the nanocrystals also show excellent biocompatibility based on MTT assays shown in Figure S16, demonstrating their good potentials in cellular imaging.

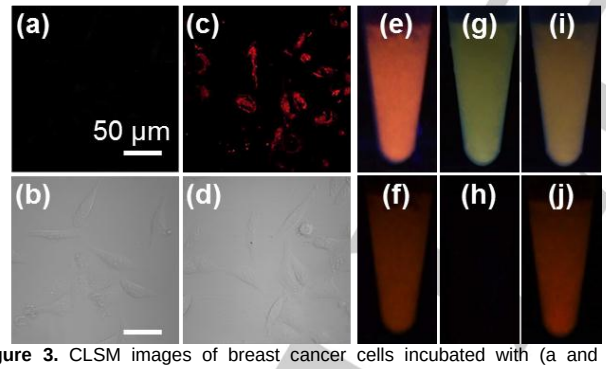

Figure 3. CLSM images of breast cancer cells incubated with (a and b) amorphous nanoaggregates, (c and d) nanocrystals of C-C4-Br; breast cancer cells incubated with (e) C-C4-Br nanocrystals (UV on), (f) C-C4-Br nanocrystals (UV off), (g) fluorescein (UV on), (h) fluorescein (UV off), (i) C-C4-Br nanocrystals and fluorescein (UV on), (j) C-C4-Br nanocrystals and fluorescein (UV off).

In conclusion, a pure organic persistent RTP compound with bright red phosphorescence was designed and synthesized. The high brightness was mainly due to the IEC and intermolecular heavy atom effect as a result of the introduction of a free chain linker in the molecular design, which significantly enhances the intermolecular interaction between the head of one molecule and the tail of the adjacent one. To successfully bring the molecule into aqueous media, nanocrystals with an average size of 180 nm were prepared, which showed bright phosphorescence in aqueous media with excellent biocompatibility. The nanocrystals were directly applied for imaging of breast cancer cells, showing effective uptake and bright phosphorescence emission. This study opens new opportunities to further explore the application of purely organic persistent RTP compounds in biological world.

Acknowledgements

The authors are grateful to the Singapore National Research Foundation (R279-000-444-281 and R279-000-483-281), the National University of Singapore (R279-000-482-133), Institute of Materials Research and Engineering of Singapore (IMRE/13-8P1104), NSFC (21672267, 51473185, 51603232 and 61605253), 863 Program (SS2015AA031701), Science and Technology Planning Project of Guangdong (2015B090913003) and the Fundamental Research Funds for the Central Universities.

Keywords: organic materials • persistent room temperature phosphorescence • nanocrystals • bioimaging

[1] S. R. Forrest, M. A. Baldo, D. F. O'Brien, Y. You, A. Shoustikov, S. Sibley, M. E. Thompson, *Nature* **1998**, *395*, 151.
[2] A. Kishimura, T. Yamashita, K. Yamaguchi, T. Aida, *Nat Mater* **2005**, *4*, 546.
[3] G. Marriott, R. M. Clegg, D. J. Arndt-Jovin, T. M. Jovin, *Biophys. J.* **1991**, *60*, 1374.
[4] O. Bolton, K. Lee, H. J. Kim, K. Y. Lin, J. Kim, *Nat Chem* **2011**, *3*, 205.
[5] S. Mukherjee, P. Thilagar, *Chem Commun (Camb)* **2015**, *51*, 10988.
[6] Z. An, C. Zheng, Y. Tao, R. Chen, H. Shi, T. Chen, Z. Wang, H. Li, R. Deng, X. Liu, W. Huang, *Nat Mater* **2015**, *14*, 685.
[7] S. Kuno, H. Akeno, H. Ohtani, H. Yuasa, *Phys Chem Chem Phys* **2015**, *17*, 15989.
[8] P. Xue, J. Sun, P. Chen, P. Wang, B. Yao, P. Gong, Z. Zhang, R. Lu, *Chem Commun (Camb)* **2015**, *51*, 10381.
[9] C. Li, X. Tang, L. Zhang, C. Li, Z. Liu, Z. Bo, Y. Q. Dong, Y.-H. Tian, Y. Dong, B. Z. Tang, *Advanced Optical Materials* **2015**, *3*, 1184.
[10] Y. Gong, G. Chen, Q. Peng, W. Z. Yuan, Y. Xie, S. Li, Y. Zhang, B. Z. Tang, *Adv Mater* **2015**, *27*, 6195.
[11] Z. Yang, Z. Mao, X. Zhang, D. Ou, Y. Mu, Y. Zhang, C. Zhao, S. Liu, Z. Chi, J. Xu, Y. C. Wu, P. Y. Lu, A. Lien, M. R. Bryce, *Angew Chem Int Ed Engl* **2016**, *55*, 2181.
[12] S. Xu, R. Chen, C. Zheng, W. Huang, *Adv Mater* **2016**, *28*, 9920.
[13] Y. Liu, G. Zhan, Z.-W. Liu, Z.-Q. Bian, C.-H. Huang, *Chin. Chem. Lett.* **2016**, *27*, 1231.
[14] T. Itoh, *Chem. Phys. Lett.* **1988**, *151*, 166.
[15] S. Scypinski, L. J. C. Love, *Anal. Chem.* **1984**, *56*, 322.
[16] W. Z. Yuan, X. Y. Shen, H. Zhao, J. W. Y. Lam, L. Tang, P. Lu, C. Wang, Y. Liu, Z. Wang, Q. Zheng, J. Z. Sun, Y. Ma, B. Z. Tang, *The Journal of Physical Chemistry C* **2010**, *114*, 6090.
[17] D. Lee, O. Bolton, B. C. Kim, J. H. Youk, S. Takayama, J. Kim, *J Am Chem Soc* **2013**, *135*, 6325.
[18] X. Chen, C. Xu, T. Wang, C. Zhou, J. Du, Z. Wang, H. Xu, T. Xie, G. Bi, J. Jiang, X. Zhang, J. N. Demas, C. O. Trindle, Y. Luo, G. Zhang, *Angew Chem Int Ed Engl* **2016**, *55*, 9872.
[19] H. Shi, Z. An, P.-Z. Li, J. Yin, G. Xing, T. He, H. Chen, J. Wang, H. Sun, W. Huang, Y. Zhao, *Crystal Growth & Design* **2016**, *16*, 808.
[20] Y. Gong, Y. Tan, H. Li, Y. Zhang, W. Yuan, Y. Zhang, J. Sun, B. Z. Tang, *Science China Chemistry* **2013**, *56*, 1183.
[21] H. Wang, H. Wang, X. Yang, Q. Wang, Y. Yang, *Langmuir* **2015**, *31*, 486.
[22] V. Martinez-Martinez, R. Sola Llano, S. Furukawa, Y. Takashima, I. Lopez Arbeloa, S. Kitagawa, *Chemphyschem* **2014**, *15*, 2517.
[23] G. Zhang, J. Chen, S. J. Payne, S. E. Kooi, J. N. Demas, C. L. Fraser, *J Am Chem Soc* **2007**, *129*, 8942.
[24] X. Sun, X. Wang, X. Li, J. Ge, Q. Zhang, J. Jiang, G. Zhang, *Macromol. Rapid Commun.* **2015**, *36*, 298.
[25] A. Fermi, G. Bergamini, R. Peresutti, E. Marchi, M. Roy, P. Ceroni, M. Gingras, *Dyes and Pigments* **2014**, *110*, 113.
[26] J. Xu, A. Takai, Y. Kobayashi, M. Takeuchi, *Chem Commun (Camb)* **2013**, *49*, 8447.
[27] G.-P. Yong, Y.-M. Zhang, W.-L. She, Y.-Z. Li, *J. Mater. Chem.* **2011**, *21*, 18520.
[28] X. Chen, C. Xu, T. Wang, C. Zhou, J. Du, Z. Wang, H. Xu, T. Xie, G. Bi, J. Jiang, X. Zhang, J. N. Demas, C. O. Trindle, Y. Luo, G. Zhang, *Angewandte Chemie* **2016**, *128*, 10026.
[29] S. M. Fateminia, Z. Wang, C. C. Goh, P. N. Manghnani, W. Wu, D. Mao, L. G. Ng, Z. Zhao, B. Z. Tang, B. Liu, *Adv Mater* **2017**, *29*, 1604100.
[30] P. Xue, P. Wang, P. Chen, B. Yao, P. Gong, J. Sun, Z. Zhang, R. Lu, *Chem. Sci.* **2016**.

10.1002/anie.201705945

WILEY-VCH

COMMUNICATION

A bright pure organic compound with red persistent room temperature phosphorescence is synthesized. Its nanocrystals show excellent biocompatibility, water dispersity and retaining bright phosphorescence in aqueous media, which show great potentials in bioimaging.

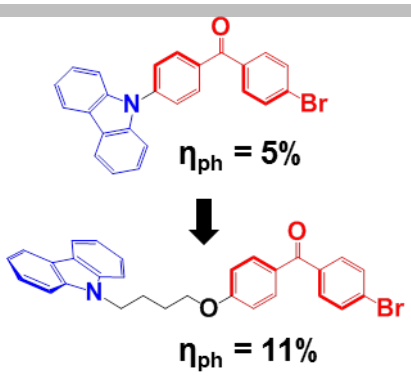

S. M. Ali Fateminia, Zhu Mao, Shidang Xu, Zhiyong Yang, , Zhenguo Chi, Bin Liu

Page No. – Page No.
Organic Nanocrystals with Bright Red Persistent Room-Temperature Phosphorescence for Biological Applications